Improving the Transient Performance in Robotics Force Control using Nonlinear Damping

Chow Yin Lai

***Abstract*— Robotics force control is increasingly being used in the manufacturing industry, to perform surface polishing, deburring, parts mating etc. However, to avoid the high impact force which could damage the workpiece, a common strategy is to command the robot to approach the workpiece slowly, which increases the overall cycle time. In this paper, we propose a nonlinear damping control scheme which reduces the force overshoot without compromising on the dynamic response. The controller design and the parameter tuning are relatively straightforward because of the clear physical meanings of the parameters. Finally, the effectiveness of the proposed controller is verified through simulation studies.**

I. INTRODUCTION

In recent years, industrial robots are increasingly being used to perform operations which require a contact between the robot (tool) and the workpiece, such as surface polishing, deburring and part mating [1],[2], in contrast to their "more traditional" tasks of spray painting or arc welding which require little or no contact at all. To ensure the success of the afore-mentioned contact-type operations, robotics force control is crucial because it not only prevents excessive contact force which could damage the workpiece, but also regulates the machining force to obtain a consistent surface quality or smoothened edge across the whole workpiece.

Various force control algorithms have been proposed in the academia over the past four decades, such as stiffness and impedance control [2],[3],[4],[5],[6], as well as the hybrid position/force control and parallel force/position control approach which deal with simultaneous position and force tracking in different directions [5],[7],[8],[9],[10]. Based on these algorithms, some major industrial robot manufacturers such as ABB, FANUC and KUKA have also started offering force-controlled robotic manipulators into the market.

Even though the topic of force control has been researched for many years, it can be noticed that the transient response of the contact force has not been given much attention. To prevent excessive force overshoot which could damage the delicate workpiece, the common approach is to design a controller which gives the overall closed loop system a large damping. The force response will indeed be smooth, but the drawback is that overall response will be slow. Since it takes a long time for the desired force to be achieved before the process of polishing or deburring can be started, the productivity of the process will be negatively affected.

This work was supported by the Science and Engineering Research Council, Agency for Science, Technology and Research (A*STAR) under Grant U12-R-051SU / SIMT / 12-410025.

The author is with A*STAR Singapore Institute of Manufacturing Technology (SIMTech), 71 Nanyang Drive, Singapore 638075 cylai@simtech.a-star.edu.sg

The cases where the robot (tool) initially moves in free space and then comes into contact with the workpiece is even more challenging. If the velocity of the manipulator just before and at the instance of impact is large, the impact force can be extremely high, leading to chattering, which means the robot would bounce back and the tool would lose contact with the workpiece [11],[12],[13],[14]. In a similar spirit to tuning a high damping, one common approach to overcome the high impact force problem is to approach the workpiece with the optimal velocity [14]. However, this 'optimal velocity' could still be too slow from the user's point of view, resulting in a loss of productivity, especially if the process is repeated many times per day.

In view of the above issues, it can be concluded that there is a need to speed up the force response while avoiding high impact force or force overshoot. Besides expensive mechanical re-design of the robotic manipulator, the use of advanced control scheme is also an attractive solution. The composite nonlinear feedback (CNF) control technique, comprising a linear feedback law which yields a closed loop system with low damping for a quick response, and a nonlinear feedback law which increases the damping ratio while the output approaches the target reference in order to reduce the overshoot caused by the linear part, is a viable option. It was initially proposed by [15] and has gained a large popularity in the hard disk drive community, where an accurate positioning of the read-write head must be achieved within a time of less than one millisecond with no overshoot [16],[17]. More recently, the CNF technique is also used for position control of robotic manipulators [18].

Motivated by the above development, we have proposed a CNF-like nonlinear damping controller to improve the transient performance of a single degree-of-freedom (DOF) actuator [19]. Here we would like to extend the algorithm for a multi-DOF robotic manipulator, showing that the algorithm can ensure the contact force reach the target value rapidly with minimal overshoot. Even in the multi-DOF setting, the design of the nonlinear damping is straightforward and the parameters have clear physical meaning, allowing a simple tuning or calculation. The effectiveness of the proposed controller is then validated in simulation studies.

This paper is organized as follows: In Section II, the details of the nonlinear damping controller for application on a multi-DOF robotic manipulator are given, followed by a stability analysis in Section III. Section IV shows the simulation results of the proposed nonlinear damping controller. The paper ends with conclusions in Section V.

II. CONTROL DESIGN FOR MULTI-DOF ROBOT

A. System Equation

Consider the dynamic model of a robotic manipulator in contact with the environment as follows:

$$M(q)\ddot{q} + C(q,\dot{q}) + G(q) = \tau - J^T F_s \quad (1)$$

where q, $\dot{q}$, $\ddot{q}$ are the joint position, velocity and acceleration vectors respectively, $M(q)$ is the inertia matrix, $C(q,\dot{q})$ is the vector of centrifugal and Coriolis terms, and $G(q)$ is a vector of gravity terms. Moreover, τ is a vector of the joint torques, F_s is a vector of the external contact forces in Cartesian coordinates (for e.g., for a 6-axis force/torque sensor, $F_s = [F_x, F_y, F_z, \tau_x, \tau_y, \tau_z]^T$), and J is the Jacobian matrix which maps Cartesian forces into equivalent joint torques. All the aforementioned matrices are common in robotics literature and thus are not elaborated here.

The model of the contact force F_s is

$$F_s = K_f(p_e - p_0). \quad (2)$$

where p_0 represents the position and orientation of a point on the undeformed surface of the workpiece, p_e is the position and orientation of the end-point of the robot / tool, and K_f represents the translational and rotational stiffness of the workpiece. A two-dimensional example of this is shown in fig. 1, where the model of the translational portion of F_s is

$$F_{xy} = K_{f,t}(p_{e,t} - p_{0,t}) \quad (3)$$

and the model of the rotational portion of F_s, i.e. the torque, is

$$\tau_z = K_{\tau,z}(p_{e,r} - p_{0,r}). \quad (4)$$

Also shown in fig. 1 is that F_{xy} is the resultant of $k_{f,x}(p_{e,x} - p_{0,x})$ and $k_{f,y}(p_{e,y} - p_{0,y})$. Throughout this paper, it is assumed that the workpiece is homogeneous, such that $K_{f,t}$ is the same in all directions. This also ensures that the direction of $p_e - p_0$ is normal to the workpiece surface.

B. Innermost Linearization and Compensation Loop

Next, the control design is detailed. First of all, the innermost linearization and compensation loop is designed as:

$$\tau = M(q)\alpha + C(q,\dot{q}) + G(q) + J^T F_s \quad (5)$$

which leads to:

$$\ddot{q} = \alpha \quad (6)$$

where α is a control signal. Since the aim is to control the force in the task space, α is designed as:

$$\alpha = J^{-1}(a - \dot{J}(q,\dot{q})\dot{q}) \quad (7)$$

where a is another control signal from the position loop, which will be described next. In actual fact, a is also the task space acceleration command calculated from the joint velocity, as can be seen by substituting equation (7) into (6):

$$a = J\ddot{q} + \dot{J}\dot{q} = \frac{d(J\dot{q})}{dt} = \frac{dv}{dt} = \frac{d^2 p_e}{dt^2} \quad (8)$$

where p_e is a vector of the task space position and orientation.

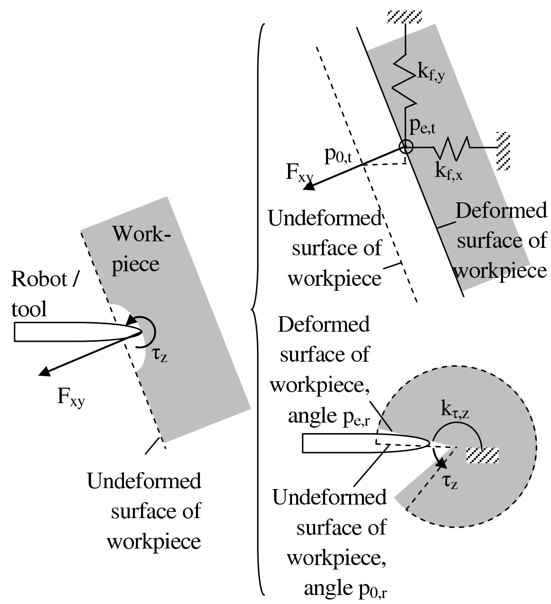

Fig. 1. Model of the translational contact force

C. Inner Position Loop

The inner position controller is designed as:

$$a = \ddot{p}_e = \ddot{p}_r + K_{Dp}(\dot{p}_r - \dot{p}_e) + K_{Pp}(p_r - p_e) \quad (9)$$

where p_r is the reference task-space position given by the outer loop's force control which is to be designed later. This gives:

$$(\ddot{p}_r - \ddot{p}_e) + K_{Dp}(\dot{p}_r - \dot{p}_e) + K_{Pp}(p_r - p_e) = 0 \quad (10)$$

which guarantees p_e approaches p_r for all positive definite K_{Dp} and K_{Pp}. These parameters are assigned such that p_e approaches p_r rapidly, for e.g. 5 times faster than the outer force loop. For simplicity, K_{Dp} and K_{Pp} can be designed as diag$(k_{Dp1}, k_{Dp2}, ...)$ as well as diag$(k_{Pp1}, k_{Pp2}, ...)$ respectively so that each parameter is associated with one single DOF.

D. Outer Force Loop - Nonlinear Controller Design

Now, the design of the force controller for the outermost loop is presented. A linear force controller can be given as:

$$K_{Ap}\ddot{p}_r + K_{Vp}\dot{p}_r = F_r - F_s \quad (11)$$

where F_r is the vector of desired forces/torques in task space coordinates. The force controller controls the contact force by changing the reference position p_r. For example, if the contact force F_s is less than the desired value F_r, p_r will be increased in the direction of the workpiece so that the tool pushes harder/deeper into the workpiece, until the desired force is achieved. Here, K_{Ap} and K_{Vp} are also designed as diagonal matrices diag$(k_{Ap1}, k_{Ap2}, ...)$ and diag$(k_{Vp1}, k_{Vp2}, ...)$ for convenience. The entries of these two matrices are delibrately chosen such that the closed loop system has a low damping and thus rapid response.

To reduce the overshoot in contact force without sacrificing the rapid response, a nonlinear damping is added to the controller:

$$K_{Ap}\ddot{p}_r + (K_{Vp} + \rho(\cdot))\dot{p}_r = F_r - F_s \tag{12}$$

with

$$\rho(F_r, F_s) = \mathrm{diag}(\rho_1(F_{r1}, F_{s1}), \rho_2(F_{r2}, F_{s2}), ...) \tag{13}$$

The question now is how this nonlinear damping should look like. The answer to this question lies in what is to be achieved using this additional damping. Firstly, when the contact force F_{si} is still far from the desired value F_{ri}, the nonlinear damping should have minimal effect so that overall, the linear low damping controller causes a rapid response. Then, only when F_{si} approaches F_{ri}, albeit with a high possibility of overshoot, the nonlinear damping should start to be injected into the system in order to reduce the overshoot. It is also desirable that the nonlinear function to be smooth. One simple nonlinearity with the desired characteristics would be the Gaussian function:

$$\rho_i(F_{ri}, F_{si}) = \alpha_i e^{-\dfrac{(F_{si} - F_{ri})^2}{2(\sigma_i \cdot F_{ri})^2}} \tag{14}$$

or

$$\rho_i(F_{ri}, F_{si}) = \alpha_i e^{-\dfrac{(F_{si})^2}{2(\sigma_i)^2}} \tag{15}$$

if F_{ri} is zero, to avoid division by zero.

In equations (14) and 15), α_i represents the additional damping which is added into the closed loop system when $F_{si} = F_{ri}$, whereas $\sigma_i \cdot F_{ri}$ determines when the nonlinear damping starts becoming significant. σ_i is scaled by F_{ri} in order to ensure that the force response is similar for different values of reference forces. The clear physical meanings help to simplify the tuning of these parameters.

III. STABILITY ANALYSIS

In this section, the stability of the closed loop system under the proposed control scheme is analyzed. Firstly, it is noted that the inner position loop is stable for all positive definite K_{Dp} and K_{Pp}. Therefore, as long as the input to this inner position loop (i.e. reference position signal, which is equivalent to the output of the force controller) is bounded, the actual position will also be bounded. With this, the internal stability of the system is not a concern for the stability analysis of the outer loop. Furthermore, because K_{Dp} and K_{Pp} have been chosen such that p_e approaches p_r rapidly, for e.g. 5 times faster than the outer force loop, it is assumed that $p_e = p_r$ from the viewpoint of the slower outer loop.

To proceed with the stability proof, the following assumption is made:

Assumption 1: The geometry of the contact plane is known. This allows a reasonable reference force to be specified. For e.g. in fig. 1, if the gradient of the workpiece with respect to the x and y axis is minus 10, then $p_{e,x} - p_{0,x}$ will definitely be 10 times larger than $p_{e,y} - p_{0,y}$. Since it is assumed that the workpiece is homogeneous, we must specify the reference value of F_x to be 10 times larger than F_y. Otherwise, the both the force values cannot be achieved simultaneously. Then, if the control parameters are the same in all axes, the end-point of the robot/tool will automatically move in the direction normal to the workpiece surface. With this, p_0 will remain constant throughout the force control process.

Since p_0 is a constant due to Assumption 1, $\dot{p}_0$ and $\ddot{p}_0$ are both zero. Therefore:

$$\dot{F}_s = K_f(\dot{p}_e) \tag{16}$$

$$\ddot{F}_s = K_f(\ddot{p}_e) \tag{17}$$

Next, because p_e is assumed to be p_r from the viewpoint of the slower outer force loop, thus $\dot{p}_e = \dot{p}_r$ and $\ddot{p}_e = \ddot{p}_r$, giving:

$$\dot{F}_s = K_f(\dot{p}_r) \tag{18}$$

$$\ddot{F}_s = K_f(\ddot{p}_r) \tag{19}$$

The force controller was designed as:

$$K_{Ap}\ddot{p}_r + (K_{Vp} + \rho(\cdot))\dot{p}_r = F_r - F_s \tag{20}$$

Using equations (18) and (19), the closed loop equation of force becomes:

$$K_{Ap}K_f^{-1}\ddot{F}_s + (K_{Vp} + \rho(\cdot))K_f^{-1}\dot{F}_s = F_r - F_s \tag{21}$$

which can be written as:

$$\begin{aligned}\underbrace{\begin{bmatrix} \dot{F}_s \\ \ddot{F}_s \end{bmatrix}}_{\dot{x}} &= \underbrace{\begin{bmatrix} 0 & I \\ -K_f K_{Ap}^{-1} & -K_f K_{Ap}^{-1} K_{Vp} K_f^{-1} \end{bmatrix}}_{A_{\text{lin}}} \underbrace{\begin{bmatrix} F_s \\ \dot{F}_s \end{bmatrix}}_{x} \\ &+ \underbrace{\begin{bmatrix} 0 \\ K_f K_{Ap}^{-}1 \end{bmatrix}}_{B} F_r \\ &- \underbrace{\begin{bmatrix} 0 & 0 \\ 0 & K_f K_{Ap}^{-1} \rho(\cdot) K_f^{-1} \end{bmatrix}}_{A_{\text{nonlin}}} \underbrace{\begin{bmatrix} F_s \\ \dot{F}_s \end{bmatrix}}_{x}\end{aligned} \tag{22}$$

or

$$\dot{x} = A_{\text{lin}}x + BF_r - A_{\text{nonlin}}x \tag{23}$$

To proceed with the stability proof, the following assumption is made:

Assumption 2: The linear force controller, without the additional nonlinear damping, asymptotically stabilizes the system, i.e. $\dot{x} = A_{\text{lin}}x + BF_r$ is asymptotically stable. Equivalently, there exist a positive definite matrix Q such that for $V = x^T x$,

$$\begin{aligned}\dot{V} &= x^T(A_{\text{lin}} + A_{\text{lin}}^T)x + 2x^T BF_r \\ &\leq -x^T Qx.\end{aligned} \tag{24}$$

This assumption is reasonable as the linear controller would have already been designed to asymtotically stabilize the system.

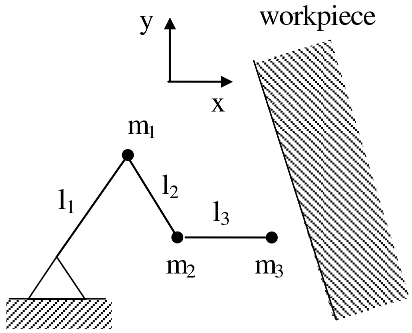

Fig. 2. 3-link robot used in simulation

Next, when the nonlinear damping is added into the system, for $V = x^T x$, the derivative would be:

$$\begin{aligned}\dot{V} = &\underbrace{x^T(A_{\text{lin}} + A_{\text{lin}}^T)x + 2x^T B F_r}_{\leq -x^T Q x \text{ by Assumption 2}} - x^T(A_{\text{nonlin}} + A_{\text{nonlin}}^T)x \\ &\leq -x^T Q x - x^T(A_{\text{nonlin}} + A_{\text{nonlin}}^T)x \end{aligned} \tag{25}$$

Because matrices K_f, K_{Ap} are positive definite, and since $\rho(\cdot)$ is Gaussian and is always greater than zero, the matrix $(A_{\text{nonlin}} + A_{\text{nonlin}}^T)$ is positive semi-definite. This means that $\dot{V}$ remains negative. Therefore, it can be concluded, from equation (25), that the closed loop system with the additional nonlinear damping remains asymptotically stable.

IV. SIMULATION RESULTS

A. Simulations

Simulations were carried out to verify the effectiveness of the proposed nonlinear damping controller. Consider a three-link planar manipulator as shown in Fig. 2. For simplicity, the mass distribution is assumed to be extremely simple: All mass exists as a point mass at the distal end of each link, and they are labeled as m_1, m_2 and m_3 respectively.

The model of the manipulator is in the form:

$$M(q)\ddot{q} + C(q, \dot{q}) + G(q) = \tau - J^T F_s \tag{26}$$

where $q = [q_1, q_2, q_3]^T$, $\tau = [\tau_1, \tau_2, \tau_3]^T$, and $F_s = [F_x, F_y, \tau_z]^T$. The matrices $M(q)$, $C(q, \dot{q})$ and $G(q)$ can be derived using Lagrangian dynamics, whereas J can be calculated from the relationship between joint velocities and task space velocities. The parameters of the robotic system are given in TABLE I.

The manipulator is initially not touching the workpiece, and the goal is to establish a contact and then maintain the forces at $F_x = F_{xr}$, $F_y = F_{yr}$ and $\tau_z = 0$. As pointed out in Section III, it is assumed that the gradient of the workpiece is known, and therefore an achievable ratio for F_{xr} and F_{yr} is given. It can thus be expected that the manipulator moves in the way as shown in Figs. 3 and 4, i.e. the manipulator will first move towards the workpiece along the surface normal, and then reorient itself such that the measured τ_z becomes zero.

Three different scenarios are studied in the simulation study with different goals in mind:

TABLE I

PARAMETERS OF THE SIMULATED ROBOTIC SYSTEM

Parameter	Symbol	Value	Unit
Mass of link 1	m_1	10	kg
Mass of link 2	m_2	8	kg
Mass of link 3	m_3	6	kg
Length of link 1	l_1	1	m
Length of link 2	l_2	0.8	m
Length of link 3	l_3	0.6	m
Workpiece translational stiffness	$k_{f,x}$	10000	N/m
Workpiece translational stiffness	$k_{f,y}$	10000	N/m
Workpiece rotational stiffness	$k_{\tau,z}$	50	N/m

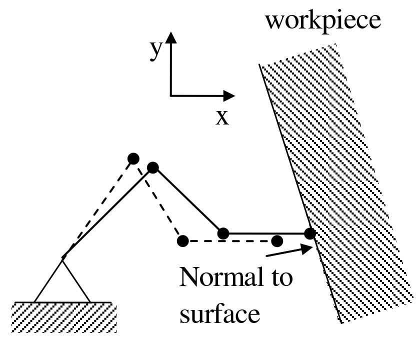

Fig. 3. Robot establishing contact with workpiece

1) Firstly, we design a linear controller, by defining the values of $K_{Ap} = I_{3\times3}$ and $K_{Vp} = 150 I_{3\times3}$ such that the closed loop system has high damping. For this controller, we would expect a force response with minimal overshoot, but the settling time could be unacceptably long.
2) Next, keeping the same K_{Ap} as in item 1, a new set of K_{Vp} is designed such that the closed loop system has a much lower damping. Here, K_{Vp} is set as $20 I_{3\times3}$. The expected force response would be rapid, but this comes at the expense of excessive overshoot.
3) Finally, we move on to design the nonlinear damping controller. The values of K_{Ap} and K_{Vp} are the same as in item 2, whereas the Gaussian nonlinearity which increases the system's damping in the vicinity of the reference values, and thus reduce the overshoot, has the parameters $\alpha = 400$ and $\sigma = 0.3$.

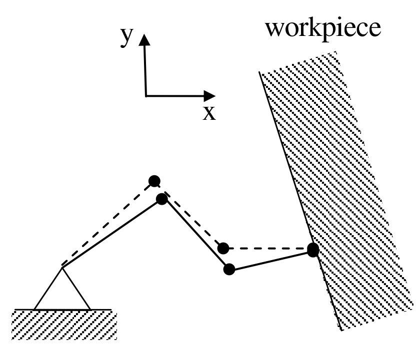

Fig. 4. Robot rotates to be perpendicular to workpiece

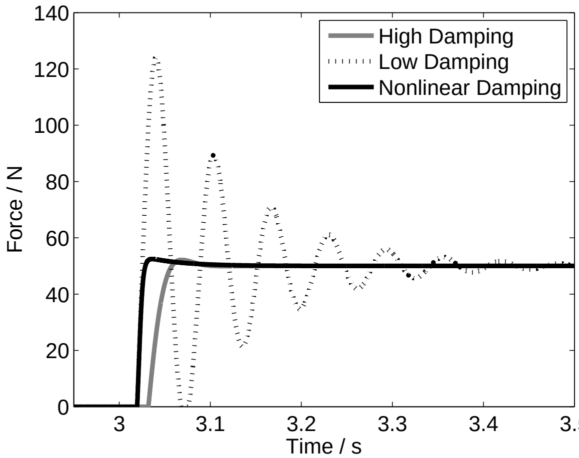

Fig. 5. F_x response

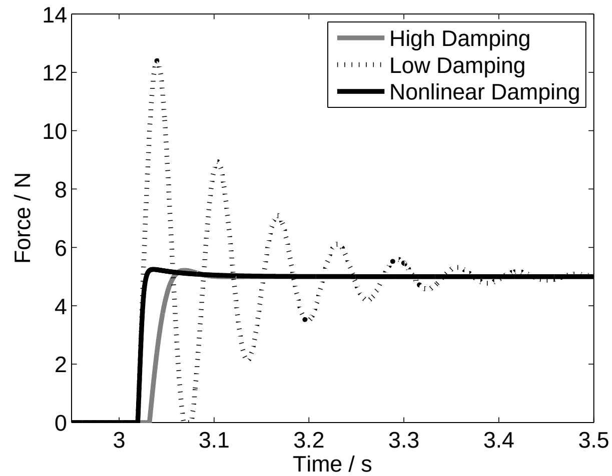

Fig. 6. F_y response

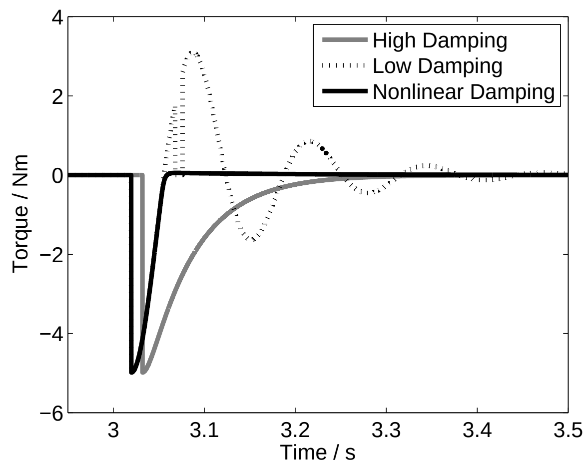

Fig. 7. τ_z response

The simulation results for F_x and τ_z are shown in Figs. 5, 6 and 7 respectively. It can be observed that in the case of high damping, the contact forces/torque start at a later time as compared to the low and nonlinear damping case. This is because the higher damping results in a slower approach speed, and the manipulator takes a longer time to reach the surface of the workpiece even though the manipulator is at the same distance from the workpiece for all three simulations. The high damping case thus indeed has a low force overshoot, but the overall response time (including approaching the workpiece and reaching the desired value) is long. On the other hand, the approach speed is faster when a low damping is tuned for the system. However, the overshoot and oscillations are excessive and would not be accepted in practical applications. Finally, the nonlinear damping controller gives good results both in terms of response time and overshoot. The approach speed and force response follows the low damping case at the initial stage, before the gaussian term becomes significant. Then, in the vicinity of desired values, the gaussian damping becomes larger and this prevents the force to shoot up to a much higher value.

From the simulation results, it can be concluded that the nonlinear damping controller indeed provides the best transient response, having a fast rise time and fast settling time with no or reduced overshoots, which cannot be achieved simultaneously using purely linear controllers.

B. Discussions

The previous remark on "...best transient response...which cannot be achieved simultaneously using purely linear controllers" deserves some elaboration. It is actually possible to retune K_{Ap} while keeping $K_{Vp} = 150I_{3\times3}$, equivalent to increasing the bandwidth while maintaining the high damping, to obtain similar approach speed as given by the low damping and nonlinear damping controller in the previous simulations. However, it is worth noting that with the newly tuned K_{Ap}, it is then always possible to find yet another smaller K_{Vp} and gaussian damping parameters to get an even faster response with minimal overshoot. Thus, there is always a nonlinear damping controller which can outperform a purely linear controller.

Next, it is also noted that currently, another approach to obtain fast force control response is by using variable compliance actuators. However, the two approaches are not mutually exclusive. By using a nonlinear damping controller on a variable compliance actuators, an even faster response with good transient can be expected.

V. CONCLUSIONS

In this paper, a nonlinear damping controller is proposed to improve the transient performance of the contact/machining force between a robot and a workpiece. Firstly, a linear controller is designed such that the force closed loop system has a low damping, which would make the system very responsive to changes in the reference value. To prevent overshoot and oscillatory behavior associated with low damping, a nonlinear damping is then added to the closed loop system as the contact force approaches the desired value. This additional nonlinear damping can be tuned easily as its parameters possess clear physical meaning. The effectiveness of the proposed controller in providing a fast response with minimal overshoot is verified through simulations. Future work includes performing more simulation studies on 6 degrees-of-freedom manipulator and redundant manipulator, as well as verifying the control algorithm through experimental studies.

VI. ACKNOWLEDGMENTS

The author gratefully acknowledges the contribution of the Agency of Science, Technology and Research (A*STAR) and reviewers' comments.

REFERENCES

[1] S. Chiaverini, B. Siciliano, and L. Villani, "A Survey of Robot Interaction Control Schemes with Experimental Comparison," *IEEE/ASME Transactions on Mechatronics*, Vol. 4, No. 3, 1999, pp. 273-285.

[2] R. Johansson and A. Robertson, "Robotic Force Control using Observer-based Strict Positive Real Impedance Control," in *Proc. IEEE International Conference on Robotics and Automation*, Taiwan, 2003, pp. 3686-3691.

[3] J. K. Salisbury, "Active Stiffness Control of a Manipulator in Cartesian Coordinates," in *Proc. IEEE Conference on Decision and Control*, Albuquerque, NM, 1980, pp. 95-100.

[4] N. Hogan, "Impedance Control: An Approach to Manipulation, Parts I-III," *ASME Journal of Dynamic Systems, Measurement, and Control*, Vol. 107, 1985, pp. 1-24.

[5] R. J. Anderson and M. W. Spong, "Hybrid Impedance Control of Robotic Manipulators," *IEEE Journal of Robotics and Automation*, Vol. 4, No. 5, 1988, pp. 549-556.

[6] M. Dohring and W. Newman, "Admittance Enhancement in Force Feedback of Dynamic Systems," in *Proc. IEEE International Conference on Robotics and Automation*, Washington DC, 2002, pp. 638-643.

[7] M. H. Raibert and J. J. Craig, "Hybrid Position / Force Control of Manipulators," *ASME Journal of Dynamic Systems, Measurement, and Control*, Vol. 103, 1981, pp. 126-133.

[8] M. T. Mason, "Compliance and Force Control for Computer Controlled Manipulators," *IEEE Transactions on Systems, Man, and Cybernetics*, Vol. 6, 1981, pp. 418-432.

[9] O. Khatib, "A Unified Approach for Motion and Force Control of Robot Manipulators: The Operational Space Formulation," *IEEE Journal of Robotics and Automation*, Vol. 3, No. 1, 1987, pp. 43-53.

[10] S. Chiaverini and L. Sciavicco, "The Parallel Approach to Force/Position Control of Robotic Manipulators," *IEEE Transactions on Robotics and Automation*, Vol. 9, 1993, pp.361-373.

[11] K. Youcef-Toumi and D. A. Gutz, "Impact and Force Control," in *Proc. IEEE International Conference on Robotics and Automation*, Scottsdale, AZ, 1989, pp. 410-416.

[12] I. D. Walker, "The Use of Kinematic Redundancy in Reducing Impact and Contact Effects in Manipulation," in *Proc. IEEE International Conference on Robotics and Automation*, Cincinnati, OH, 1990, pp. 434-439.

[13] R. Volpe and P. Khosla, "Experimental Verification of a Strategy for Impact Control," in *Proc. IEEE International Conference on Robotics and Automation*, Sacramento, California, 1991, pp. 1854-1860.

[14] K. Kitagaki and M. Uchiyama, "Optimal Approach Velocity of End-Effector to the Environment," in *Proc. IEEE International Conference on Robotics and Automation*, Nice, France, 1992, pp. 1928-1934.

[15] Z. Lin, M. Pachter, and S. Banda ,"Towards Improvement of Tracking Performance - Nonlinear Feedback for Linear Systems," *International Journal of Control*, Vol. 70, No. 1, 1998, pp. 1-11.

[16] B. M. Chen, T. H. Lee, K. Peng, and V. Venkataramanan, "Composite Nonlinear Feedback Control for Linear Systems with Input Saturation: Theory and an Application," *IEEE Transactions on Automatic Control*, Vol. 48, No. 3, 2003, pp. 427-439.

[17] W. Lan, C. K. Thum, and B. M. Chen, "A Hard-Disk Drive Servo System Design using Composite Nonlinear Feedback Control with Optimal Nonlinear Gain Tuning Methods," *IEEE Transactions on Industrial Electronics*, Vol. 57, No.5, 2010, pp. 1735-1745.

[18] W. Peng, Z. Lin, and J. Su, "Computed Torque Control-based Composite Nonlinear Feedback Controller for Robot Manipulators with Bounded Torque," *IET Control Theory and Applications*, Vol. 3, No. 6, 2009, pp. 701-711.

[19] C. Y. Lai, Y. Li, N. D. Vuong, T. M. Lim, C. Y. Ma, and C. W. Lim, "Nonlinear Damping for Improved Transient Performance in Robotics Force Control," in *Proc. IEEE International Conference on Advanced Intelligent Mechatronics*, KaoHsiung, Taiwan, 2012, pp. 314-319.

[20] S. D. Eppinger and W. Seering ,"On Dynamic Models of Robot Force Control," in *Proc. IEEE International Conference on Robotics and Automation*, 1986, pp. 29-34.